Comparison of Control Techniques in a Weight Lifting Exoskeleton

Irving Rosales-Díaz[1], Jesus Ricardo López-Gutiérrez[2*], Angel Eduardo Zamora Suárez[1], Sergio Rosario Salazar[2], Antonio Osorio-Cordero[1], Hipólito Aguilar-Sierra[3], Rogelio Lozano[1,4]

1. *CINVESTAV, Av. Instituto Politécnico Nacional 2508, Col. San Pedro Zacatenco, 07360, Mexico City, Mexico*
2. *CONACYT-CINVESTAV, Av. Instituto Politécnico Nacional 2508, Col. San Pedro Zacatenco, 07360, Mexico City, Mexico*
3. *Polytechnic University of Tulancingo, St. Ingenierias 100, Col. Huapalcalco, 43629, Tulancingo, Hidalgo, Mexico*
4. *Centre de Recherches de Royalieu, UTC-HEUDIASyC, Compiegne, 60205, France*

Abstract

The back pain is the most common injury in human activities where heavy objects must be lifted or must be suspended for a long time. A weight lifting exoskeleton also known as force augmentation exoskeleton is designed to reduce the strain on the back and the limbs and reduce the risk to suffer injuries. On the other hand, different kinds of controllers have been implemented to achieve whit this goal, for example, a conventional PD Control, PD Control with Gravity Compensation, PD Control with Adaptive Desired Gravity Compensation and PD Control with Robust Compensator. This paper aims to evaluate and compare the performance from the previously cited controllers used to reduce the strain in the back, through the implementation of each controller in a three Degrees Of Freedom (DOF) exoskeleton powered by pneumatic muscle actuators; some numerical simulations as well as experimental trials have been conducted and three different performance indices were used in order to determine the effectiveness of each one with respect to the simple PD controller when the mass to be lifted is unknown.

Keywords: augmenting force device, exoskeleton robot, pneumatic artificial muscles, adaptive control, robust control

1 Introduction

The back injuries are very common in human activities where heavy loads must be lifted or must be suspended for a long time, such as automotive assembly lines in manufacturing process, construction industry or search and rescue task to help people who are in distress like an earthquake. A Weight Lifting Exoskeleton also called Force Augmentation Exoskeleton is designed to allow the operator performing his activities with the same human's agility paying more attention in reducing the strain in the back and the limbs. The exoskeleton's actuators should supply enough force to lift the heavy load or tool for a long period of time and the human provides the necessary motions commands; reducing the risk of injuries. On the other hand, we can find in the literature that different kind of actuators and controllers have been implemented to achieve this goal, for example, in the case of hydraulic actuators we found Refs. [1] and [2]. In Ref. [1], an adaptive robust force control is designed for a 1 Degree Of Freedom (DOF) exoskeleton to solve the force augmentation problem in a human leg. In

Ref. [2], a motion control based is proposed using a torque switching control for mobility augmentation of a 4-DOF lower extremity exoskeleton. In the case of electronic actuators we have the Agri-Robot[3] which is a robotic exoskeleton developed to assist farmers in the transportation of heavy goods. The iT-Knee[4] is an active exoskeleton with a torque control scheme for torque augmentation in the knee articulation for adult people to stand up from a sitting position. Another special type of electronic actuator is the Serial Elastic Actuator (SEA). This kind of actuator incorporates the motion intention sensor in the same device, as can be seen in Ref. [5], where a force-based control is used in a 3-DOF lower limb exoskeleton to power the knee and the ankle. Kim and Bae presented a lower limb exoskeleton powered by rotary SEA. They introduce a model-inverse time delay control to generate a virtual reference to improve the performance from force-based control. The BLEEX exoskeleton[7] is powered by pneumatic actuators. It is one of the first exoskeleton that allows walking with a payload of 34 kg and was developed by the U.C. Berkeley for military marching. The Nurse Robot Suit[8]

***Corresponding author:** Jesus Ricardo López-Gutiérrez*
E-mail: rrricardooolopez@gmail.com

is a full body exoskeleton designed to assist nurse's labor lifting patients and avoid back injuries. A special kind of pneumatic devices are the Pneumatic Artificial Muscle (PAM) which have a very good weight/force ratio feature, since they can produce a lifting force up to 70 N with an actuator's weight about of 80 g. Ref. [9] describes a 2-DOF arm exoskeleton with PAM that allows moving a 4 kg object from different positions. They used a control scheme considering biomechanical properties from the human arm. Ref. [10] presents two pairs of PAMs in antagonist configuration powering a knee exoskeleton introducing a variable stiffness control scheme for muscle activation based on electromyography (EMG) analysis to evaluate the human assistance. More recently an adaptive Radial Basis Function (RBF) neural network is proposed in Ref. [11] to improve the tracking error in a lower limb exoskeleton controlled by a simple PD control with gravity compensation through a virtual torque control.

Finally, in Ref. [12] a comparison study of control algorithms is developed using a generalized model for a human wearing an exoskeleton to determine their qualitative advantages and disadvantages. The goal of this work is to evaluate and compare quantitatively the performance of various controllers used to reduce the strain in the back. Each controller was applied in a 3-DOF exoskeleton powered by PAM. Some numerical simulations as well as experimental trials have been conducted and three different performance indices were used in order to determine the effectiveness of each one with respect to a simple PD controller when the mass to be lifted is unknown.

This paper is organized as follows: In section **2** the exoskeleton's dynamical model is given. In section **3** a summary of control techniques applied to exoskeleton are presented. Section **4** describes the numerical simulations results and the performance indices are defined. Section **5** the experimental results for the hip joint are presented. Finally, the conclusions of this work are given in section **6**.

2 Modelling of the exoskeleton

The exoskeleton is modeled over the sagittal plane as shown in Fig. 1a. The coefficients involved in the modelling are: l_i (i =1, 2, 3) the lengths of leg, thigh and

spine respectively; l_{c_j} (j =1, 2, 3) are lengths from the ankle, knee and hip joints to the center of mass related to l_i respectively; the masses m_i (i =1, 2, 3) are known and m_4 is unknown due to the object.

The model was obtained employing the Euler-Lagrange approach[13] and analyzing the exoskeleton platform over the sagittal plane.

The position of the center of mass respect to jth link of an articulated arm and mass 4 positions is given by:

$$\begin{cases} x_j = \sum_{i=1}^{j-1} l_i \cos(\Theta_i) + l_{c_j} \cos(\Theta_j)[1-\delta_{nj}] \\ y_j = \sum_{i=1}^{j-1} l_i \sin(\Theta_i) + l_{c_f} \sin(\Theta_j)[1-\delta_{nj}] \end{cases}, \quad (1)$$

For our case of study $n = 4$, and δ_{in} is the Kronecker's Delta defined as:

$$\delta_{ij} = \begin{cases} 1 & \text{if} \quad i=j \\ 0 & \text{if} \quad i \neq j \end{cases} \quad \text{and} \quad \Theta_i = \sum_{j=0}^{i} \theta_j.$$

Differentiating (1) twice to obtain the acceleration, *i.e.*

$$\begin{cases} \ddot{x}_j = -\sum_{i=1}^{j} \ddot{\theta}_i \left\{ l_{c_f} \sin(\Theta_j)[1-\delta_{nj}] + \sum_{s=i}^{j-1} l_s \sin(\Theta_s) \right\} \\ \quad + \dot{\theta}_i^2 \left\{ l_{c_f} \cos(\Theta_j)[1-\delta_{nj}] + \sum_{s=i}^{j-1} l_s \cos(\Theta_s) \right\} \\ \quad + 2\dot{\theta}_i \sum_{p=i+1}^{j} \dot{\theta}_p \left[l_{c_f} [1-\delta_{nj}] \cos(\Theta_j) + \sum_{s=p}^{j-1} l_s \cos(\Theta_s) \right] \\ \ddot{y}_j = -\sum_{i=1}^{j} \ddot{\theta}_i \left\{ l_{c_f} \cos(\Theta_j)[1-\delta_{nj}] + \sum_{s=i}^{j-1} l_s \cos(\Theta_s) \right\} \\ \quad - \dot{\theta}_i^2 \left\{ l_{c_f} \sin(\Theta_j)[1-\delta_{nj}] + \sum_{s=i}^{j-1} l_s \sin(\Theta_s) \right\} \\ \quad - 2\dot{\theta}_i \sum_{p=i+1}^{j} \dot{\theta}_p \left[l_{c_f} [1-\delta_{nj}] \sin(\Theta_j) + \sum_{s=p}^{j-1} l_s \sin(\Theta_s) \right] \end{cases},$$

$$(2)$$

The following differentiations are necessary for applying Euler-Lagrange formula:

$$\begin{cases} \dfrac{\partial \dot{x}_j}{\partial \dot{\theta}_\alpha} = -u(j-\alpha)l_{c_f} \sin(\Theta_j)[1-\delta_{nj}] + \sum_{s=\alpha}^{j-1} l_s \sin(\Theta_s) \\ \dfrac{\partial \dot{y}_j}{\partial \dot{\theta}_\alpha} = u(j-\alpha)l_{c_f} \cos(\Theta_j)[1-\delta_{nj}] + \sum_{s=\alpha}^{j-1} l_s \cos(\Theta_s) \end{cases}, \quad (3)$$
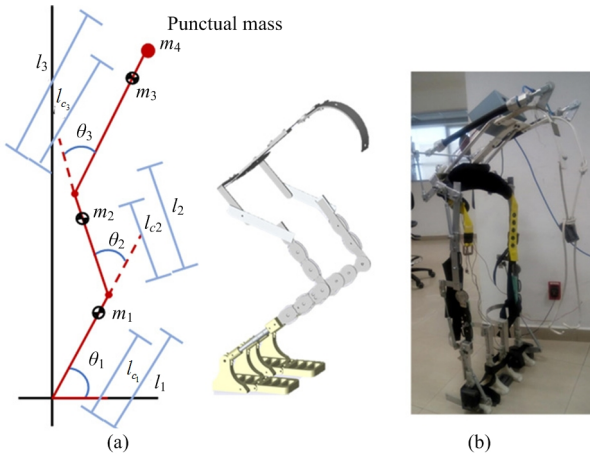
Fig. 1 (a) Free-body diagram of the exoskeleton with 3DOF; (b) structure of the exoskeleton suit.

where $u(\alpha) = \begin{cases} 1 & \text{if} \quad \alpha \geq 0 \\ 0 & \text{other case} \end{cases}$.

Notice that, we can demonstrate that,

$$\frac{\partial \dot{x}_j}{\partial \theta_x} = \frac{\mathrm{d}}{\mathrm{d}t} \frac{\partial \dot{x}_j}{\partial \dot{\theta}_x} \quad \text{and} \quad \frac{\partial \ddot{y}_j}{\partial \theta_x} = \frac{\mathrm{d}}{\mathrm{d}t} \frac{\partial \ddot{y}_j}{\partial \dot{\theta}_x}$$

Finally, it was computing the gravitational torques as:

$$\frac{\partial y_i}{\partial \theta_\alpha} = \sum_{i=\alpha}^{j-1} l_i \cos(\Theta_i)$$
$$+ l_{c_j}(1 - d_{nj}) \cos(\Theta_j) u(j - \alpha). \tag{4}$$

In general, the movement equations according to Euler-Lagrange are given by:

$$\tau_i = \frac{\mathrm{d}}{\mathrm{d}t} \frac{\partial L}{\partial \dot{\theta}} - \frac{\partial L}{\partial \theta_i}$$
$$= \sum_{i=1}^{n} m_j \left\{ \ddot{x}_j \frac{\partial \dot{x}_j}{\partial \dot{\theta}_i} + \ddot{y}_j \frac{\partial \ddot{y}_j}{\partial \dot{\theta}_i} \right\} + \sum_{p=i}^{n} I_p \ddot{\Theta}_p + m_p g \frac{\partial y_p}{\partial \theta_i}, \tag{5}$$

is also substituted into Eq. (5) in order to obtain a model of a 3 DOF system, where $n = 4$ is the number of mass elements and $i = 1, 2, 3, \ldots, n-1$ is the number of joints. In other words, mathematical model of the system in matrix form is,

$$M(\Theta)\ddot{\Theta} + C(\Theta, \dot{\Theta})\dot{\Theta} + g(\Theta) + f(\Theta) = \tau. \tag{6}$$

That is the dynamic equation for robots with n DOF, where the elements or entries of the matrix $M(\Theta)$ are given by Eq. (7).

In Eqs. (6) and (7), the entries of the matrix C were

obtained by Christoffel's symbols[13], as shown:

$$c_{nkj} = \begin{bmatrix} c_{1kj} \\ \vdots \\ c_{n-1kj} \end{bmatrix}^{\mathrm{T}} \begin{bmatrix} \theta_1 \\ \vdots \\ \theta_n \end{bmatrix}.$$

Taking in account, $c_{ijk} = \frac{1}{2}[Q_{kji} + Q_{kij} - Q_{jik}]$ and $Q_{\alpha j\gamma} = \partial M_{\alpha i} / \partial \theta_\gamma$.

In addition, a dynamic friction term that is a non-conservative force was added to the general model, due to the material employed in the making of the joints of the robot. The type of friction proposed is static due to the dry surfaces and it is assumed that the exoskeleton moves smoothly so Coulomb and Viscous frictions are negligible. In the case of the robot reported in this paper, the friction coefficients for aluminum are given as f_1, $f_2, \ldots, f_{(n-1)} = 1.30$.

3 Control techniques for exoskeleton suit

It will be shown the structure of PD Control, PD Control with Gravity Compensation, PD Control with Robust Compensator and PD Control with Adaptive Desire Gravity Compensation.

3.1 PD control

This controller was proposed in order to realize the first tests and it is well known as:

$$\tau = K_p e(t) + K_d \dot{e}(t), \tag{8}$$

where

$K_p = K_p^T > 0$ and $K_p \in R^{3\times3}$ is a diagonal and square matrix of proportional gains, and the position error is defined as $e = \theta_d - \theta$, where θ_d is the desired angular position and θ is the real position for ankle, knee and hip joints.

$K_d = K_d^T > 0$ and $K_d \in R^{3\times3}$ is a diagonal and square matrix of derivatives gains and velocity error is defined as $\dot{e} = \dot{\theta}_d - \dot{\theta}$.

3.2 PD Control with gravity compensation

This controller is very similar to the previous one except for the fact that gravitational torques were added to compensate the torque due to the unknown weight of the mass m_4 that is sensed by a load sensor cell. So, the controller is given by:

$$\tau = K_p e(t) + K_d \dot{e}(t) + g(\Theta). \tag{9}$$

$$M_{\alpha i} = \sum_{j=1}^{n} m_j \left\{ l_{c_j}^2 [1 - \delta_{nj}] + u[j - 1 - \max(\alpha, i)] \sum_{s=\min(\alpha, i)}^{\max(\alpha, i)-1} l_{c_j} l_s \cos(\Theta_j - \Theta_s) \right.$$

$$\left. + \sum_{s=\min(\alpha, i)}^{j-1} \left\{ l_s^2 + 2 l_{c_j} l_s [1 - \delta_{nj}] \cos(\Theta_j - \Theta_s) + \sum_{q=\min(\alpha, i)}^{\max(\alpha, i)-1} l_s l_q \cos(\Theta_s - \Theta_q) + 2 \sum_{o=s+1}^{j-1} l_o l_s \cos(\Theta_o - \Theta_s) \right\} \right\} u(j - \alpha), \quad (7)$$

The term $g(\Theta)$ involves the value of m_4 which is unknown but sensed by a load cell sensor.

3.3 PD Control with robust compensator

The PD Control with robust compensator was obtained as follows[14], from Eq. (6):

$$\ddot{\Theta} = M(\Theta)^{-1} \tau + M(\Theta)^{-1}(-C(\Theta, \dot{\Theta})\dot{\Theta} - g(\Theta) - f(\Theta)),$$
$$(10)$$

and defining

$$\rho = M(\Theta)^{-1}(-C(\Theta, \dot{\Theta})\dot{\Theta} - g(\Theta) - f(\Theta)),$$

then

$$\ddot{\Theta} = M(\Theta)^{-1} \tau + \rho.$$

The following control law was proposed,

$$u_i = M(\Theta)^{-1} \tau,$$

where $\tau = M(\Theta)(\tau_{RB} + \tau_N)$, therefore, the system is $\ddot{\Theta} = \tau_{RB} + \tau_N + \rho$, and $\tau_N = K_p e(t) + K_d \dot{e}(t)$ is the nominal PD Controller.

The robust part comes as the output of the following second order system,

$$\begin{cases} \dot{z}_{i1} = -g_i z_{i1} - g_i^2 e_{i1} + a_i^N u_i, \\ \dot{z}_{i2} = -g_i z_{i2} + z_{i1} + 2 g_i e_{i1}, \\ \tau_{RB} = g_i^2 (z_{i2} - e_{i1}) / a_i^N, \qquad i = 1, 2, 3 \end{cases} \quad (11)$$

$g_i (i = 1, 2, 3)$ are the robust filter parameters of the robust compensator, z_{i1} and z_{i2} are the states obtained from a second-order robust filter, a_i^N are scalars that need to be large and positive, in other hand, $e_{i1} (i = 1, 2, 3)$ are the errors for each joint; ankle, knee and hip respectively.

3.4 PD Control with adaptive desired gravity compensation

The control was designed according to Ref. [13] and is the following:

$$\tau = K_p e(t) + K_d \dot{e}(t) + \Phi_g(\Theta_d)\hat{\varphi}(t) + g_0(\Theta_d), \quad (12)$$

the estimator is proposed as:

$$\hat{\varphi}(t) = \Gamma \Phi_g(\Theta_d)^{\mathrm{T}} \int_0^t \left[\frac{\varepsilon_0}{1 + \|e(t)\|} e(t) - \dot{e}(t) \right] ds + \hat{\varphi}(0), \quad (13)$$

where $K_p, K_d \in \mathbf{R}^{n \times n}$ and $\Gamma = \Gamma^{\mathrm{T}} \in \mathbf{R}^{m \times m}$ are symmetric positive definite design matrices, on other hand, $\hat{\varphi}(t) \in \mathbf{R}^m$ is the estimation vector and $\hat{\varphi}(0) \in \mathbf{R}^m$ is the initials conditions vector for the estimator. Furthermore, $\Phi_g(\Theta_d) \in \mathbf{R}^{n \times m}$ is the matrix that contains term affected by the unknown parameter and $g_0(\Theta_d) \in \mathbf{R}^n$ is the nominal gravity vector and includes the terms no affected by φ (unknown parameter m_4).

for our platform,

$$\Phi_g(\Theta_d) = \begin{bmatrix} g(l_1 \cos(\theta_1)) + l_2 \cos(\theta_1 + \theta_2) + l_3 \cos(\theta_1 + \theta_2 + \theta_3) \\ g(l_2 \cos(\theta_1 + \theta_2) + l_3 \cos(\theta_1 + \theta_2 + \theta_3)) \\ g l_3 \cos(\theta_1 + \theta_2 + \theta_3) \end{bmatrix}.$$

4 Simulation results

When employing Eq. (12) to perform PD control with adaptive compensation, the estimated parameter, which is the unknown mass to be lifted, is obtained from the estimator Eq. (13). However, when dealing with the problem of the lifting a mass and transporting it somewhere, it is necessary to give in Eq. (13) a value to $\hat{\varphi}(0)$. If any value is given to $\hat{\varphi}(0)$, the initial tracking error might be large because the estimator does not have yet enough data to give a good estimate. To sort out this disadvantage, the action is divided into two stages. In the first stage, it was considering a constant reference and unknown constant mass $m_4 = 1$ kg $i.e.$ a regulation problem was solved in order to get an estimate of the known parameter. In a second stage, the estimated value in first stage was used as the initial condition $\hat{\varphi}(0)$ of the estimator to solve the tracking problem with the best performance.

In Fig. 2, the results of a regulation problem are presented. This problem was performed with the aim of getting an estimate of the value of the unknown parameter mass "m_4"($\hat{\varphi}(t)$) that will be employed later as an initial condition for the estimator Eq. (13) when solving a tracking problem. Fig. 3 shows the results of the estimated parameter after the regulation problem was solved.

The results of the tracking problem during lifting exercise of an unknown weight when a PD, PD control with gravity compensation, PD control with robust compensator and a PD control with adaptive desired gravity compensation can be seen in Fig. 4, where Θ_d represents the desired trajectory of the angular position for ankle, knee and hip joints.

The error signal which is defined as the difference between the desired and real angular positions is displayed in Fig. 5 for each control and articulated available joint.

The performance indexes for each controller were computed[15]. Let $e(t)$ be the error signals of the system, when applying any of the proposed controllers and let $e(t)_{ad}$, $e(t)_{rb}$, $e(t)_{pd}$ and $e(t)_{pdg}$ be the error signals when using the adaptive control and the other respectively.

The performance indices of the system are defined as follows:

Integral of the Absolute Error (IAE)

$$\eta_{\text{IAE}} = \int_0^\infty |e(t)\mathrm{d}t|.$$

Integral of Time by Absolut Error (ITAE)

$$\eta_{\text{ITAE}} = \int_0^\infty t|e(t)\mathrm{d}t|.$$

Integral of Square Error (ISE)

$$\eta_{\text{ISE}} = \int_0^\infty e(t)^2 \mathrm{d}t.$$

In Table 1, we can see that PD control with adaptive compensation is better than others proposed control laws in this work. The procedure realized with this controller allows estimating a physical unknown parameter and good performance in tracking trajectory.

Although, all the control laws are applicable to all

Table 1 Performance indices based on error signals from exoskeleton on simulation

	Joint	Performance indices	
		IAE	ITAE	ISE
PD control	Ankle	0.5576	6.401	0.02231
	Knee	1.01	8.405	0.07667
	Hip	0.6397	5.072	0.03309
PD + gravity compensation	Ankle	0.3426	3.84	0.007235
	Knee	0.6809	5.712	0.03573
	Hip	0.5282	4.626	0.0210
PD + robust compensator	Ankle	0.1829	1.927	0.002608
	Knee	0.4821	4.28	0.01722
	Hip	0.4814	5.28	0.01757
PD + adaptive compensation	Ankle	0.03636	0.3554	8.984×10^{-5}
	Knee	0.13	1.273	0.001134
	Hip	0.1007	1.001	0.0006527

robotic joints, they were shown only the graphs that represent the performance behavior of the control laws applied only in the hip joint in order to compare with experimental results and performance indices, see Figs. 6 – 8.

5 Experimental results

Tests were carried out with the experimental setup whose model was previously presented and built in our laboratory. Experimental tries consisted in manipulate the robotic hip joint by means of a given trajectory applying the controllers described previously. During the experiments, the legs of the robot were kept fixed employing passive actuators (pressure air springs). The human spine has a range of motion from 0° to 120°, for security reasons, reference motion for hip joint was constrained up to 80°, see Fig. 9. Control laws applied were divided in two independent signals, due to there are two electrovalves that control the action of inflate or deflate the pneumatic actuators.

5.1 PD control

The control law makes the system follow the desired trajectory with a considerable error ($e(t)_{pd}$). The oscillations of the system around the desired trajectory are in the range −10° up to 8°, as shown in Fig. 10.

5.2 PD Control with gravity compensation

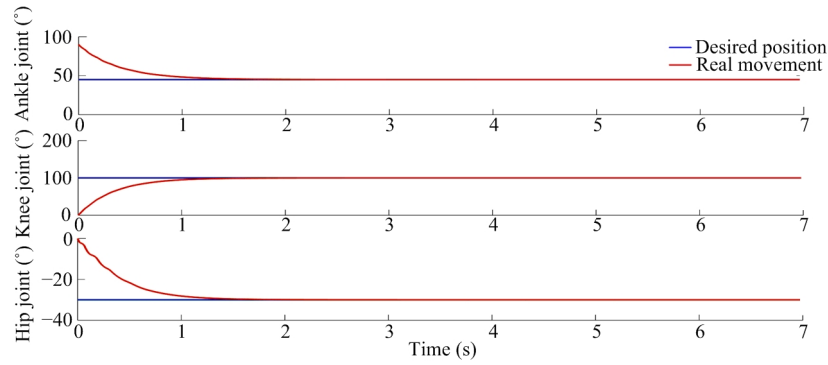A load sensor was attached to the upper structure of

Fig. 2 Signals of angular regulation position by PD control with adaptive desired gravity compensation.
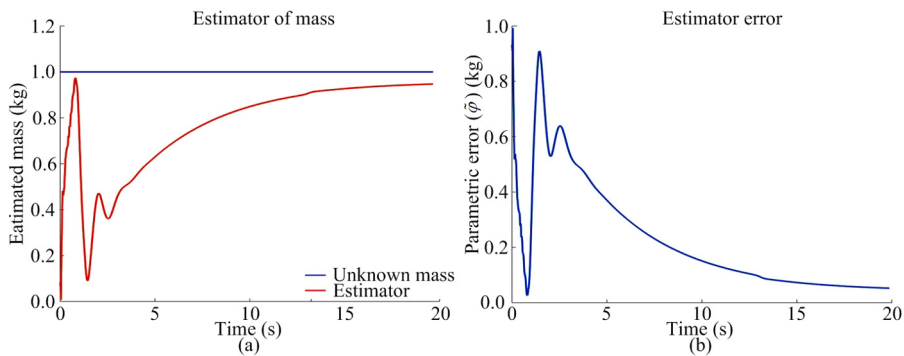

Fig. 3 Estimated mass and parametric error by means of regulation process with PD control with adaptive desired gravity compensation.
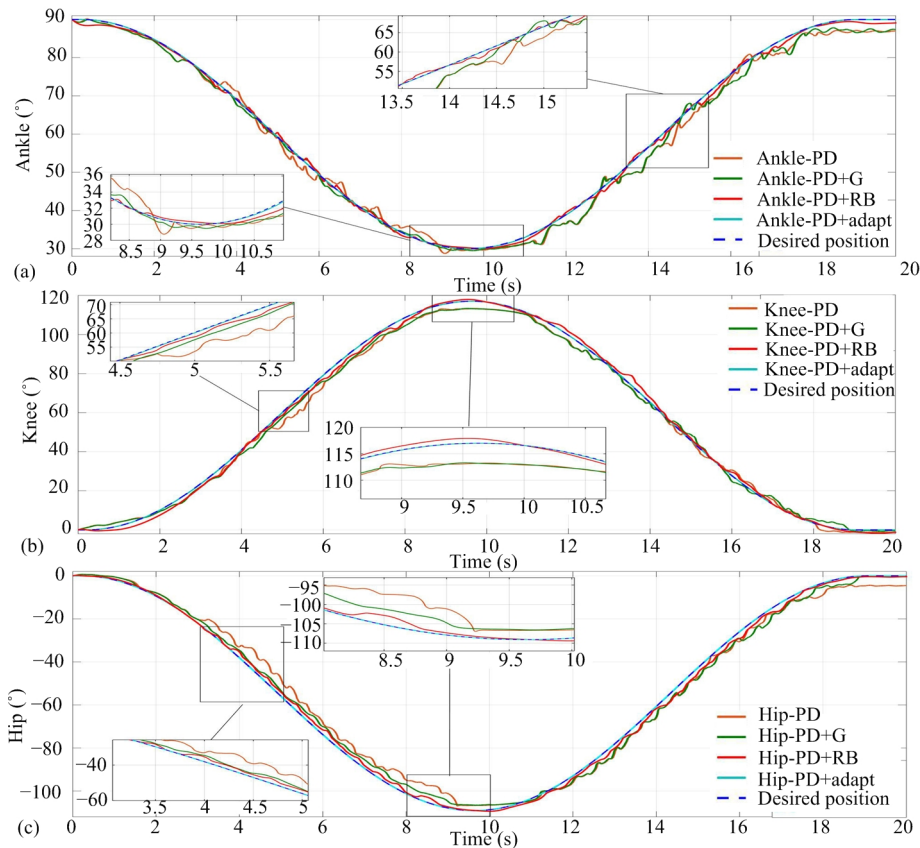

Fig. 4 Signals of angular position tracking for PD control, PD control with gravity compensation, PD control with robust compensator and PD control with adaptive desired gravity compensation were shown for: (a) ankle joint, (b) knee joint and in (c) hip joint..
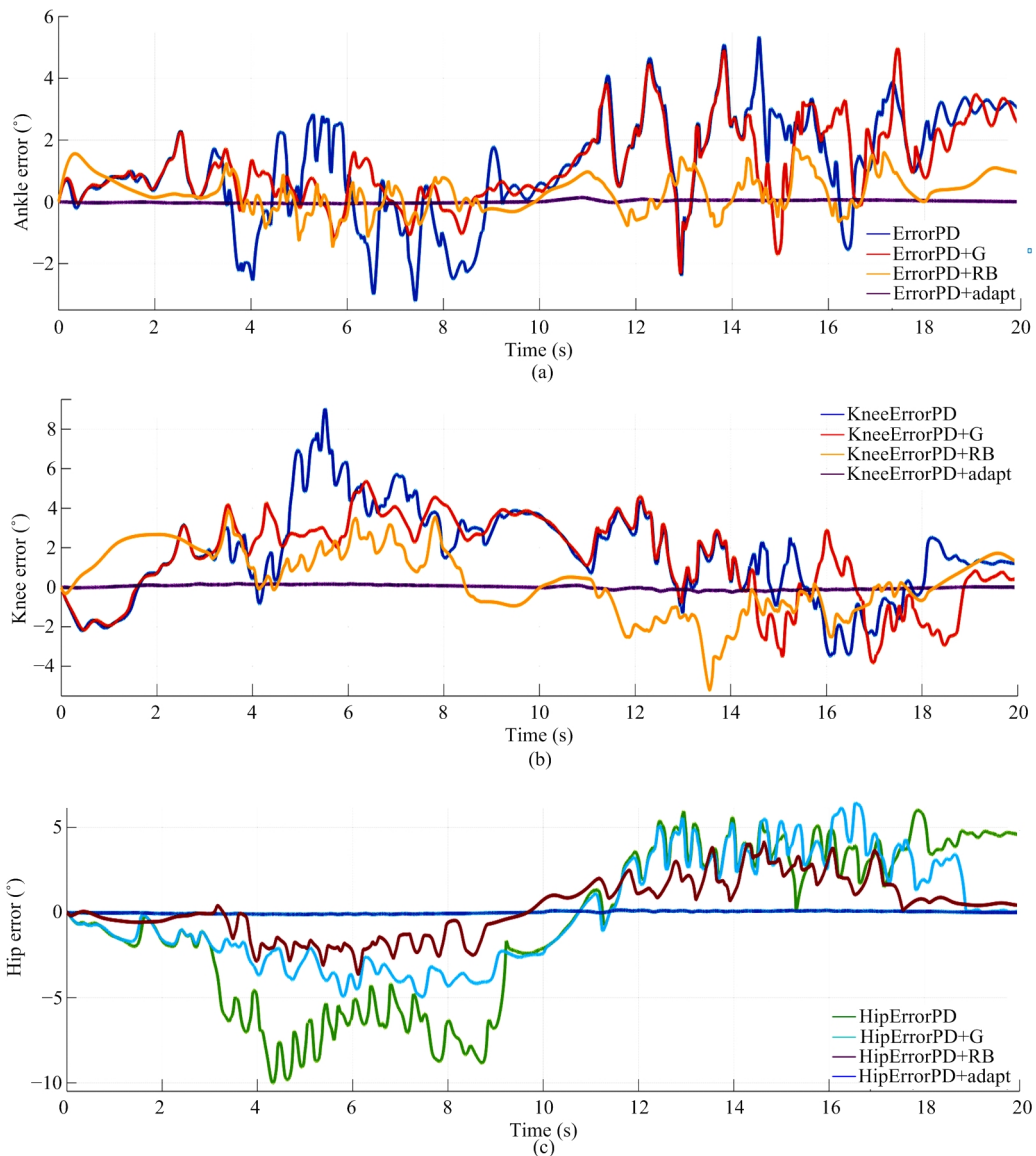
Fig. 5 Error signals for angular tracking position applied in each joint.
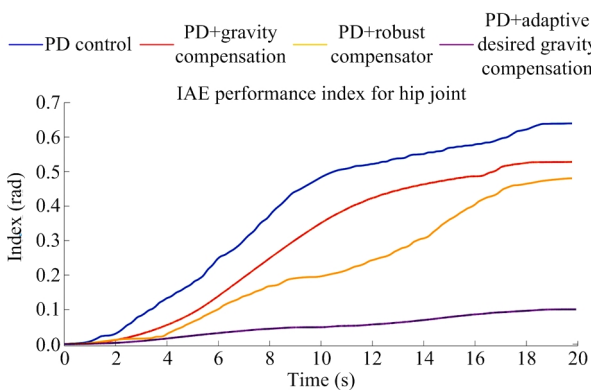
Fig. 6 Integral of the absolute error is the performance index computed only for hip joint applying all control laws on simulation.
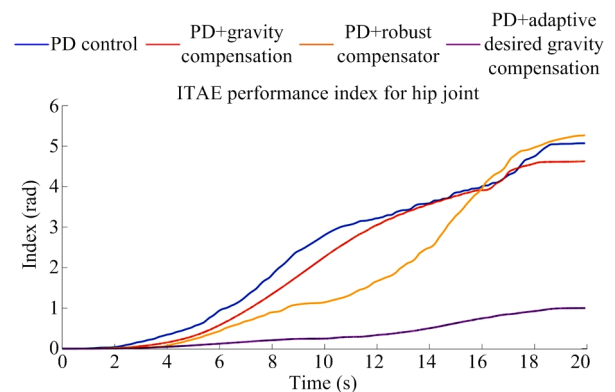
Fig. 7 Integral of time of the absolute error is the performance index computed only for hip joint applying all control laws on simulation.
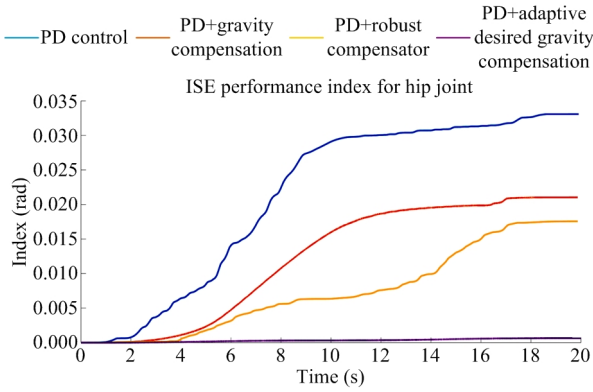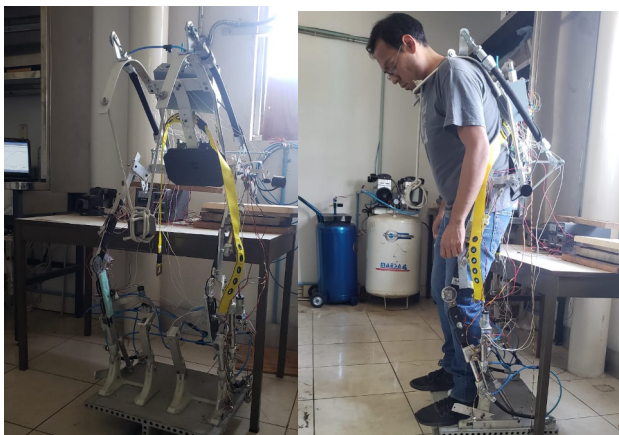
Fig. 8 Integral of square error is the performance index computed only for hip joint applying all control laws on simulation.

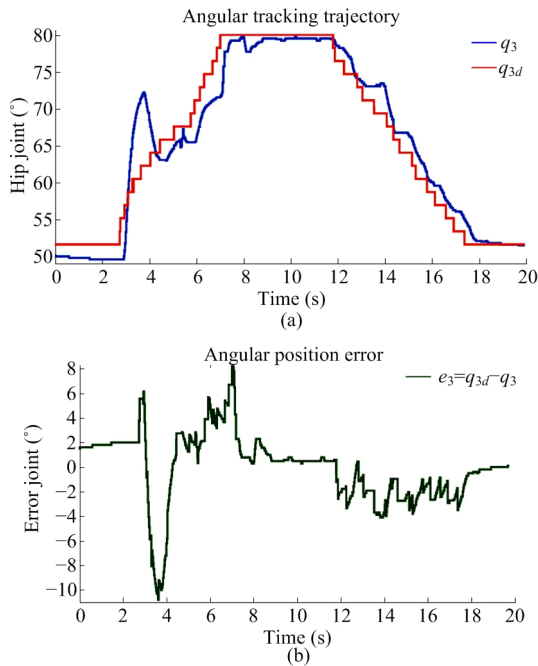Fig. 9 Exoskeleton robot suit and experimental tests.

Fig. 10 PD control for angular tracking position.

the robot in order to sense the mass of the load. The reading of the sensor is used by the controller to cancel out the effects of gravity. Fig. 11 shows the behavior of the hip joint when the user tries to reach the upright position. Hysteresis behavior is always present at the moment to activate the pneumatic artificial muscles.

5.3 PD control with robust compensation

This technique overcomes the effects of non-linearities such as friction or hysteresis, however, a suitable gain for it must be chosen. By means of trial and error were found a suitable gain, see Fig. 12. We can see that the follow up of the reference is more precise, lower energy expenditure and in this case, the error $(e(t)_{rb})$ oscillates between $-6°$ up to $6°$.

5.4 PD Control with adaptive desired gravity compensation

In this case, the procedure is similar to the corresponding simulation tests; firstly, a regulation exercise was performed an estimated initial value for $\varphi_r(t)$, see Fig. 9. The regulated position was reached after approximately 35 s. The value of φ was recorded and was
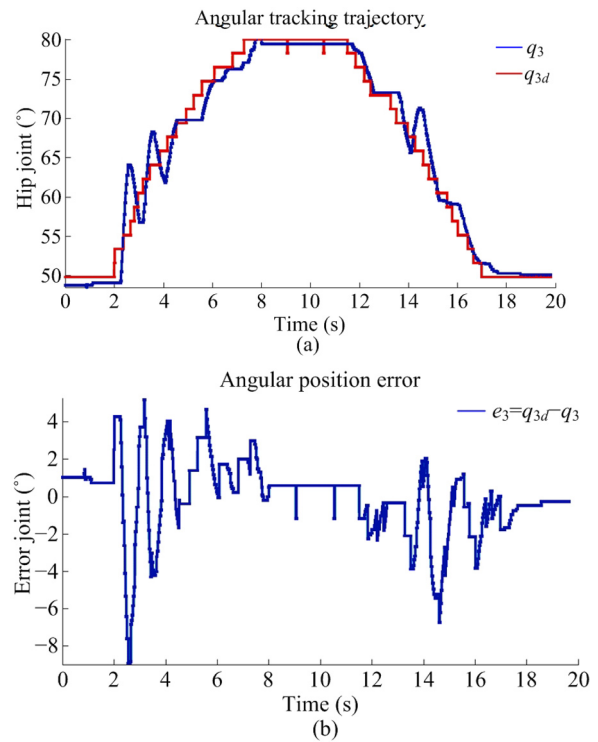

Fig. 11 PD control with gravity compensation for angular tracking position.

used as the initial data for the estimator into this controller for tracking problem. So, for the second step, initial condition for the estimator and tracking the human reference is $\varphi_t(0) = \varphi_r(t) = 0.95$ (where $\varphi_r(t)$ is the estimated parameter from regulation process and $\varphi_t(0)$ is the initial condition for the estimator on tracking process). The results corresponding to this control law for tracking trajectory are displayed in Fig. 13.

Although, this control requires more time to achieve the objective, the tracking behavior was better than the others, where θ is closer to θ_d and the error $e(t)_{ad}$ in Fig. 14b shows a reduced range of $-4°$ to $4°$.

Table 2 presents the values of the performance indexes for all controllers on experiments. The last control technique has been the best in coincidence with the simulation results.

Graphs in Fig. 15 illustrate the index performance for each control law applied for experimental results, only for the position error signal in hip joint. In Fig. 15a was shown the IAE index for each control, Fig. 15b for

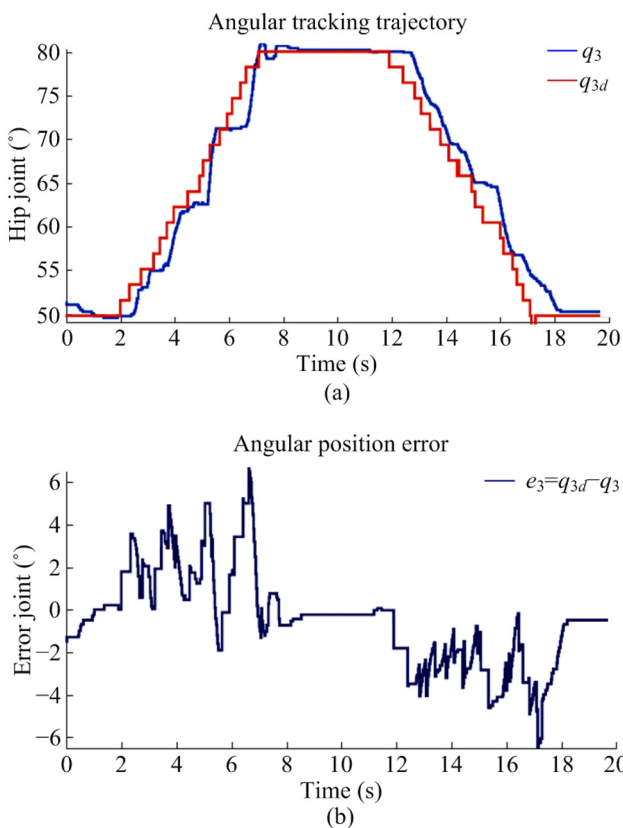ITAE index and finally Fig. 15c for ISE index. All data was converted from degrees to radians.

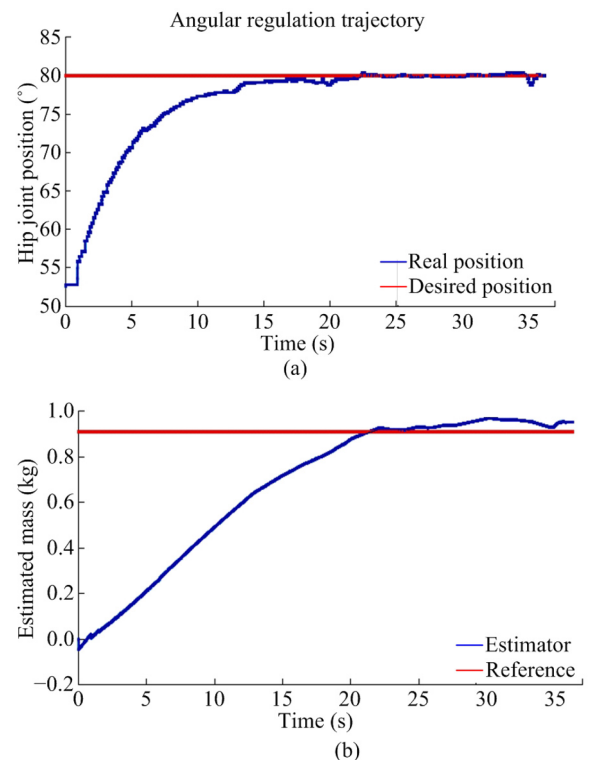**Fig. 13** Regulation position to identify and estimate the mass.

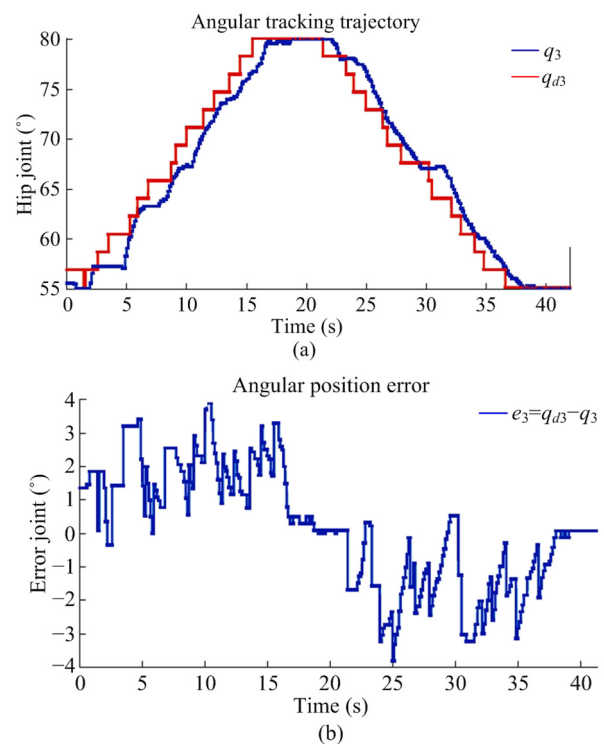**Fig. 12** PD control with robust compensator for angular tracking postion.

Fig. 14 PD control with adaptive desired gravity compensation for angular tracking position.

Table 2 Performance indices based on error signals for hip joint on experiments

		Performance indices		
	Joint	IAE	ITAE	ISE
PD	Hip	0.7255	5.861	0.0492
PD with gravity compensation	Hip	$4.954×10^{-5}$	0.000419	$2.488×10^{-6}$
PD with robust compensator	Hip	$5.68×10^{-5}$	0.000609	$2.99×10^{-6}$
PD with adaptive desired gravity compensation	Hip	1.085	19.94	0.0415
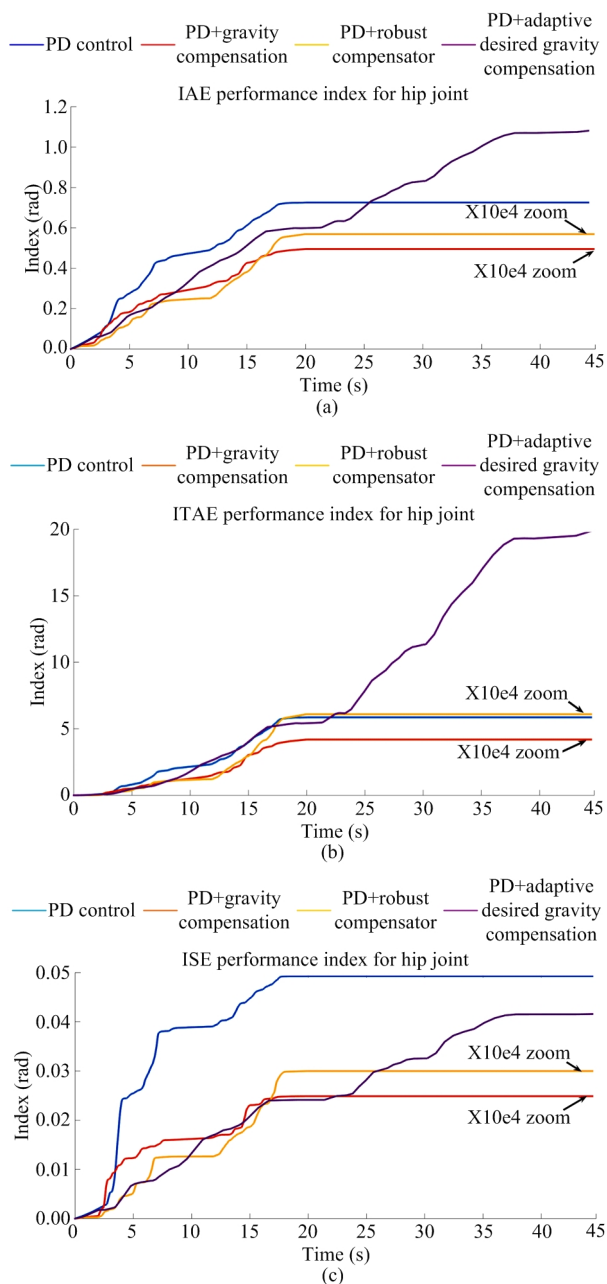
Fig. 15 Performance indexes for experimental results with each contral law applied to the exoskeleton prototype.

6 Conclusion

This project allowed the development, construction and control of an exoskeleton robot with the main objective of assisting in human activities and avoiding health problems. The control laws applied allowed us to observe several aspects to select the best option. The PD control is simple to apply since only needs information on the angular position and velocity of the controlled joint to generate the error signal. But the disadvantage lies in the fact that the tuning of the gains improves the performance only in some cases, that is, if the mass of the object to be lifted varies so it will be probable to observe an inappropriate behavior of the system may occur. In the case of the PD control with gravity compensation, the same thing happens as with the previous one. In this case, we require an extra sensor to measure the mass. PD Control with robust compensator improves the behavior of the system against non-modeled variables, does not need extra sensor information, its computational cost is low and it is easy to apply. Finally, the PD Control with adaptive compensation of the desired gravity requires knowledge of the nonlinear model, does not need extra sensor information, its computational cost and implementation is more complex that the previous controllers. According to Table 2, Fig. 15 and experimental results we conclude that PD control with gravity compensation and the robust compensator have better performances with advantages to operate and control the robot.

References

[1] Chen S, Chen Z, Yao B, Zhu X C, Zhu S Q, Wang Q F, Song Y. Adaptive robust cascade force control of 1-DOF hydraulic exoskeleton for human performance augmentation. *IEEE/ASME Transactions on Mechatronics*, 2016, **22**, 589–600.

[2] Kim H, Shin Y J, Kim J. Design and locomotion control of a

hydraulic lower extremity exoskeleton for mobility augmentation. *Mechatronics*, 2017, **46**, 32–45.

[3]   Toyama S, Yamamoto G. Development of Wearable-Agri-Robot ~ mechanism for agricultural work.# *IEEE/RSJ International Conference on Intelligent Robots and Systems*, St. Louis, MO, USA, 2009, 5801–5806.

[4]   Saccares L, Sarakoglou I, Tsagarakis N G. iT-Knee: An exoskeleton with ideal torque transmission interface for ergonomic power augmentation. *IEEE/RSJ International Conference on Intelligent Robots and Systems* (*IROS*), Daejeon, South Korea, 2016, 780–786.

[5]   Beil J, Perner G, Asfour T. Design and control of the lower limb exoskeleton KIT-EXO-1. *IEEE International Conference on Rehabilitation Robotics* (*ICORR*), Singapore, Singapore, 2015, 119–124.

[6]   Kim S, Bae J. Force-mode control of rotary series elastic actuators in a lower extremity exoskeleton using model-inverse time delay control. *IEEE/ASME Transactions on Mechatronics*, 2017, **22**, 1392–1400.

[7]   Kazerooni H, Racine J L, Huang L, Steger R. On the control of the berkeley lower extremity exoskeleton (BLEEX). *Proceedings of the IEEE International Conference on Robotics and Automation*, Barcelona, Spain, 2005, 4353–4360.

[8]   Yamamoto K, Hyodo K, Ishii M, Matsuo T. Development of power assisting suit for assisting nurse labor. *JSME International Journal Series C Mechanical Systems*, *Machine Elements and Manufacturing*, 2002, **45**, 703–711.

[9]   Goljat R, Babič J, Petrič T, Peternel L, Morimoto J. Power-augmentation control approach for arm exoskeleton based on human muscular manipulability. *IEEE International Conference on Robotics and Automation* (*ICRA*), Singapore, Singapore, 2017, 5929–5934.

[10] Maeda D, Tominaga K, Oku T, Pham H T T, Saeki S, Uemura M, Hirai H, Miyazaki F. Muscle synergy analysis of human adaptation to a variable-stiffness exoskeleton: Human walk with a knee exoskeleton with pneumatic artificial muscles. 12*th IEEE-RAS International Conference on Humanoid Robots*, Osaka, Japan, 2012, 638–644.

[11] Duong M K, Cheng H, Tran H T, Jing Q. Minimizing human-exoskeleton interaction force using compensation for dynamic uncertainty error with adaptive RBF network. *Journal of Intelligent* & *Robotic Systems*, 2016, **82**, 413–433.

[12] Concha A, González-Sánchez F E, Ramírez-Velasco E, Sánchez M, Gadi S K. Comparison of control algorithms using a generalized model for a human with an exoskeleton. *Journal of Applied Science* & *Process Engineering*, 2018, **5**, 249–255.

[13] Kelly R, Santibañez-Davila V, Loria-Perez J A. *Control of Robot Manipulators in Joint Space*. Springer, London, UK, 2005, 133–377.

[14] Liu H, Li D, Xi J, Zhong Y. Robust attitude controller design for miniature quadrotors. *International Journal of Robust and Nonlinear Control*, 2016, **26**, 681–696.

[15] Duarte-Mermoud M A, Prieto R A. Performance index for quality response of dynamical systems. *ISA Transactions*, 2004, **43**, 133–151.